MURDOCH RESEARCH REPOSITORY

http://researchrepository.murdoch.edu.au/13926/

Accepted Manuscript

Title: Electrochemical energy storage device for securing future renewable energy

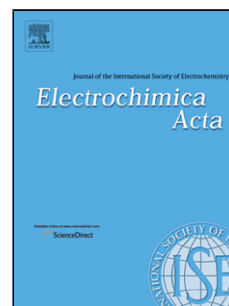Authors: Manickam Minakshi, Danielle Meyrick

Please cite this article as: M. Minakshi, D. Meyrick, Electrochemical energy storage device for securing future renewable energy, *Electrochimica Acta* (2013), http://dx.doi.org/10.1016/j.electacta.2013.02.075

Electrochemical energy storage device for securing future renewable energy

Manickam Minakshi* and Danielle Meyrick

School of Chemical and Mathematical Sciences, Murdoch University, Murdoch, WA 6150, Australia

Highlights

Aqueous rechargeable battery is suitable for stationary energy storage.

Battery was fabricated with MnO_2 cathode, Zn anode and aqueous sodium electrolyte.

Role of Na^+ cations, scan rate, degree of reduction are optimised.

Electrochemical cell exhibits high energy density, long cycle life and low cost.

Abstract

An electrochemical cell comprising molten sodium and molten sulphur as the anode and cathode respectively, with beta alumina electrolyte has never found extensive use. An approach to develop large energy storage device based on aqueous sodium electrolyte at low temperature is described. An electrochemical cell with low cost, safe and utilizing sustainable manganese dioxide (MnO_2) cathode coupled with zinc (Zn) anode in aqueous sodium hydroxide (NaOH) electrolyte is reported. The cyclic voltammetric (CV) profiles are found to be quite different in terms of peak position and current response depending on concentration of NaOH electrolyte. Among the concentrations of NaOH studied (2, 5, 7 and 10 M) the best performance was found to be between 5 and 7 M. The CV curves exhibits a pair of reversible redox peaks (within 1e$^-$ region) corresponding to sodium ion insertion and extraction but

1

while extending the potential window to second electron reduction resulted in irreversible nature. This is explained to the formation of inhomogeneous reduction reaction due to slow electron diffusion. CV experiments at various scan rates revealed that the MnO_2 material may not be suitable enough for higher scan rates indicating a sluggish kinetics occurring in the bulk material. Our study highlights the MnO_2 cathode in NaOH electrolyte features a flat discharge voltage of 1.3 V vs. Zn with discharge capacity of 220 mAh/g.

Keywords: MnO_2; aqueous; sodium; cyclic voltammetry; electrolyte.

* E-mail: minakshi@murdoch.edu.au; lithiumbattery@hotmail.com

1. Introduction

Global oil consumption is projected to increase steeply over the next two decades, creating great demand for development of alternative energy technologies. It is also well recognised that relying on fossil fuels is no longer sustainable as it is posing a serious threat to our environment. A global solution to this major challenge must involve renewable energy as an alternative source. A major barrier to wide ranging application of renewable energy sources is continuity of supply; generation of power by solar and wind sources, for example, can be hampered by time of day, dust, cloud and other weather conditions. This barrier can be most effectively overcome by large-scale energy storage systems suitable for a broad range of applications [1-2]. The approach we discuss here is the development of safe, efficient, low cost electrochemical energy storage systems that are critical to store renewable energy resources.

An electrochemical cell (battery) with high energy density enabling back up for wind and solar power, typically store low energy of between 1 and 50 KWh of energy, and have historically been based on lead-acid (Pb-acid) chemistry [3]. Pb-acid batteries are well known

2

to last for up to a decade, depending on the depth of discharge. These batteries employ highly toxic Pb and PbO_2 electrodes, and highly corrosive sulphuric acid as the electrolyte, while providing meagre energy density [4]. These issues preclude the ongoing application of this technology. There is a critical need to replace the Pb-acid battery, but high cost and safety issues of alternative battery chemistries present significant challenges. Although the lithium-ion battery is state-of-the-art for such devices, the trade-offs between performances, safety and cost have significantly hampered its utility. There is also a great concern about the cost and the potential limit of lithium resources unevenly distributed in terrestrial reserves [5-6]. The cost of lithium raw material has roughly doubled from the first practical application in 1991 to the present, and such cost may dramatically increase as the demand of lithium increases in response to large-scale energy storage applications. Therefore, alternative energy storage mechanism using abundant and environmentally friendly materials are highly desirable. In contrast to lithium resources, sodium deposits are in plenty around the world and cheap in cost [7]. Next to lithium, the electrochemical equivalent and standard potential of sodium are the most attractive and beneficial for battery applications [8]. Despite the merits of using sodium in battery systems, only a very limited number of reports are found but all are pertained to organic electrolytes [9-10]. In the present work, aqueous rechargeable $Zn|NaOH|MnO_2$ cell is demonstrated as an extension to our preliminary work reported earlier [11]. Water would represent an almost ideal alternative to the typical organic electrolytes due to a number of factors such as cost, safety, performance, and environmentally benign. In addition, the ionic conductivity of aqueous electrolytes is considerably higher than that of the non-aqueous counterparts, allowing higher C rates and lower voltage drops due to electrolyte impedance.

3

In one of our earlier work, the commercial alkaline Zn-MnO$_2$ primary cell has been transformed into a secondary cell using LiOH electrolyte [12]. In this study, a novel Zn-MnO$_2$ battery using NaOH electrolyte is explored with a special emphasis on modification in concentration of electrolyte to the existing one [11], and the effect of electrochemical performance to various scan rates and degree of reduction. The active MnO$_2$ material showed reversible intercalation of Na in MnO$_2$ suggesting the Zn|NaOH|MnO$_2$ cell could be promising for aqueous rechargeable battery system. With the aid of potentiostatic and galvanostatic techniques the electrochemical performance of the water based Zn|NaOH|MnO$_2$ cell has been optimised and discussed. The experimental evidence for the sodium insertion/extraction in host MnO$_2$ including elemental analysis and other physical characterization on the discharged/charged product is well documented in our previous study [11].

2. Experimental

The EMD (electrolytic manganese dioxide; γ-MnO$_2$) type (IBA sample 32) used in this work was purchased from the Kerr McGee Chemical Corporation. Zn foil (99.9%) from Advent research materials, zinc sulphate heptahydrate (ZnSO$_4$•7H$_2$O), and sodium hydroxide (NaOH) from Sigma Aldrich were used in this study.

The cell configuration used for potentiostatic (standard three cell electrode) is described elsewhere [13]. For cyclic voltammetric studies, MnO$_2$ was the working and zinc foil was the counter electrode, which was separated from the main NaOH electrolyte by means of a porous frit. A mercury-mercuric oxide (Hg/HgO) served as the reference electrode. Reported potentials are relative to Hg/HgO.

For galvanostatic experiments, the cells were discharged / charged galvanostatically at 0.25 mA/cm^2 on mass density (8 mA/g) by using an 8 channel battery analyzer from MTI

4

Corp., USA, operated by a battery testing system (BTS). The cut-off discharge and charge voltages were 1.0 and 1.8 V respectively. All electrochemical measurements were carried out at ambient temperature (25 ± 1° C). The MnO_2 active material was first mixed with 15 wt. % of carbon black (A-99, Asbury USA) and with 10 wt. % of poly (vinylidene di fluoride) (PVDF, Sigma Aldrich) as a binder and then pressed into a disc shape with a diameter of 12 mm. The 12 mm diameter, 0.5 mm thick electrode weighing 35 mg, containing 75% by weight of MnO_2, i.e., 26 mg has a theoretical capacity to 1.0 e^{-} discharge to Mn^{3+} of 308 $mAh.g^{-1}$. An electrochemical test cell was constructed with MnO_2 disk as the cathode, Zn metal as the anode and filter paper (Whatman filters 12) as the separator. The electrolyte used was a variety of concentrations i.e. 2, 5, 7 and 10 M of sodium hydroxide and its amount was two-fold excess to meet the amount of ions in the solution for intercalation mechanism.

3. Results and Discussion

To understand the electrochemical behaviour of MnO_2 in aqueous sodium hydroxide (NaOH) solutions, we have performed cyclic voltammetric (CV) experiments starting from 0.2 to – 0.5 V vs. Hg/HgO and then reversing it back to the starting potential. The conductivity of the MnO_2 decreases as the degree of reduction increases hence the voltametric experiments were limited to $1e^{-}$ reduction [14] for the first part of the study. We have conducted a set of experiments using NaOH electrolytes containing different concentrations such as 2, 5, 7 and 10 M. All the experiments involved MnO_2 as working and Zn as counter electrodes with a slow scan rate of 25 µV/s. The obtained CV profiles are shown in Figs.1 a-d. The electrochemical process (CV curves) comprising a set of well defined reduction (C1) and oxidation peaks (A1) of higher intensities were found in the same potential range for the moderate concentration of electrolyte (Figs. 1b-c). Especially at the

5

moderate concentration, after multiple cycles, a change in the current peak intensity was observed. However, the shape of the cyclic voltammogram of γ-MnO$_2$ appears to be similar irrespective of the electrolyte concentrations. All in all, the peak separation between C1 and A1 is larger than ideal difference (with ΔE_{pk} = 59 mV) seems to indicate a slow electron-transfer kinetics [15]. As the proposed mechanism is not a surface process like adsorption at the electrode/electrolyte interface (similar to electrochemical double layer supercapacitors) [16] but a mass transport rate occurring in bulk MnO$_2$ through intercalation, the observed peak separation is agreeable.

The CV profile in dilute NaOH electrolyte (Fig. 1a) implies that the intercalation process become more irreversible with poor current response as the Na$^+$ concentration is low. In the case of 10 M (higher) concentration (Fig. 1d), H$^+$ concentration is very low, but still a reduction and the corresponding oxidation peak is observed indicating that the Na$^+$ cation insertion and extraction into the host MnO$_2$ has been occurred. The cathodic (reduction) peak is due to the reduction of manganese ions (Mn$^{4+/3+}$) accompanied by the intercalation of sodium ions and during reversing the scan the anodic (oxidation) peak is due to the oxidation of manganese ions (Mn$^{3+/4+}$) accompanied by the deintercalation of sodium ions [11]. The process of H$^+$ insertion is not ruled out as being an aqueous (NaOH) electrolyte. The peak separation between the C1 and A1 couples decreased at higher alkaline concentrations (up to 35 mV) this could be due to that electron transfer rate dominate the overall intercalation process with higher Na$^+$ content. The intercalation and de-intercalation peaks are initially quite weak and become more pronounced say after 10-15 cycles. This may be due to the progressive interlayer expansion due to intercalation of large sodium ions which is well documented for other oxide materials [17-18]. Among the concentration studied, from Fig. 2, it could be concluded that 7 M seems to show the best performance. At a strongly caustic

6

solution (10 M NaOH) the high tendency of Na cations adsorbed on the MnO_2 electrode surface could inhibit the reversibility and hence may not be suitable for cycleability. However, all these results suggest that a reversible sodium intercalation and extraction is observed in aqueous environment and the kinetics is more pronounced when the H^+ concentration is low.

In another experiment, to investigate the influence of scan rate on the redox behaviours of MnO_2 in NaOH electrolyte, its cyclic voltammetric curves at different scan rates were recorded and their curves are plotted in Fig. 3. It can be observed from this figure that the electrode polarization increased dramatically at the higher scan rate and an increase in cathodic current with ill-defined peaks becomes essential [15]. This reveals that from lower scan to higher scan rates, the electrochemical process (insertion/extraction) changes from being kinetically nearly reversible to irreversible reactions i.e. intercalation of the sodium species in the bulk MnO_2 is not being extracted due to a slow electron transfer [19].

To investigate the extent of sodium ion intercalation the potential region was extended to second electron reduction at a lower scan rate and those result are shown in Fig. 4. There are two pair of cathodic and anodic peaks assigned as C1, C2 and A1, A2 respectively. The cathodic peak C2 appear due to inhomogeneous reduction reaction with the formation of manganese oxides such as Mn_2O_3 or Mn_3O_4 phases. As the degree of reduction has been increased, the MnO_2 has become less conductive as the electron diffusion is slow [14]. This led to the dissolution reaction which is not completely reversible as observed by the oxidation peak A2 in reversing the scan.

Galvanostatic experiments were undertaken to evaluate the discharge-charge behaviour of MnO_2 cathode in aqueous electrolyte containing 5 and 7 M electrolytes. A flooded two-electrode cell was used for this purpose and the voltage reported is against Zn

7

counter electrode. In our future publications, we will report our results based on novel phosphates, polyaniline and activated carbons as alternative anodes for aqueous rechargeable battery using Na_2SO_4 electrolyte. The discharge and charge mechanism of $Zn|NaOH|MnO_2$ cell involves sodium ion transfer from the NaOH electrolyte to the MnO_2 cathode while Zn anode forms zinc-oxyhydroxide that limits the long term cell performance. The cells containing 7 and 5 M concentration of electrolyte showed a discharge and charge voltages of 1.45/1.3 V and 1.35/1.5 V respectively. The cell containing 7 M concentration of electrolyte showed slightly a higher discharge potential but the cell capacity is found to be higher (220 mAh/g) for 5 M concentration of electrolyte. The cells containing 7 and 5 M concentration of electrolyte are shown to be fully reversible even after 40 cycles (in Fig. 5) with discharge capacities corresponding to 170 and 220 mAh/g respectively. Both the cells had an excellent cyclability of 90% capacity retention even after 40 cycles. This corresponded to an excellent efficiency after multiple cycles, exhibiting reversible electrochemical de/intercalation of sodium, making the innovative idea feasible for renewable energy storage applications. However, the cycling stability issue associated with the Zn anode need to be alleviated either by adding additives or identifying suitable anode (conducting polymers / carbon composites) that could be suitable for long term application. The bulkiness of the sodium ion relative to the lithium ion and limitation of aqueous electrolyte to 2 V may present some challenges in terms battery weight, power and footprint, this is not important for stationary, electrical grid storage applications.

4. Conclusions

An aqueous rechargeable $Zn|NaOH|MnO_2$ cell has been constructed with MnO_2 cathode, Zn anode and aqueous NaOH electrolyte. The concentration of electrolyte and its effect on MnO_2 performance was demonstrated. The mechanism of the aqueous rechargeable cell is based on

8

reduction-oxidation mechanism occurring in bulk MnO_2 rather than surface redox processes. The MnO_2 cathode is found to be safe, efficient on short-term purposes and cost effective with a reversible capacity of 220 mAh/g. The reported aqueous battery is found to be reversible during the one electron reduction and as the degree of reduction increased, cyclic voltametric curves showed that the process becomes irreversible due to the formation of non-reversible products. This research paves the way for electrochemical energy storage device that play a critical role in efforts to reduce our impact on the environment through the storage of renewable energy resources.

Acknowledgements

References

[1] D. Lindley, Nature **463** (2010) 18.

[2] J. Leadbetter and L. G. Swan, J. Power Sources **216** (2012) 376.

[3] C. P. Zhang, S. M. Sharkh, X. Li, F. C. Walsh, C. N. Zhang and J. C. Jiang, Energy Conv. and Management **52** (2011) 3391.

[4] S. Nagashima, K. Takahashi, T. Yabumoto, S. Shiga and Y. Watakabe, J. Power Sources **158** (2006) 1166.

[5] F. Risacher and B. Fritz, Aquat Geochem **15**, 123 (2009).

9

[6] A. Yaksic and J. E. Tilton, Resour. Policy **34**, 185 (2009).

[7] B. L. Ellis and L. F. Nazar, Current Opinion in Solid State Mat. Sci. **16** (2012) 168.

[8] D. Kim, S. -H. Kang, M. Slater, S. Rood, J. T. Vaughey, N. Karan, M. Balasubramanian, C. S. Johnson, Adv. Energy Mater. **1** (2011) 333.

[9] L. Arthouel, F. Moser, R. Dugas, O. Crosnier, D. Belanger and T. Brousse, J. Phys. Chem C **112** (2008) 7270.

[10] J. P. Whitacre, A. Tevar and S. Sharma, Electrochem. Commun. **12** (2010) 463.

[11] M. Minakshi, Mater. Sci. Engg. B. **177** (2012) 1788.

[12] K. Sathiyaraj, A. Pandey and M. Minakshi, Electrochim. Acta **60** (2012) 170.

[13] M. Minakshi, N. Sharma, D. Ralph, D. Appadoo, K. Nallathamby, Electrochemical and Solid- State Letters **14** (2011) A86.

[14] J. P. Brenet, J. Mallessan and A. Grund, C.R. Acad. Sci. **242** (1956) 111.

[15] N. Li, C. J. Patrissi, G. Che and C. R. Martin, J. Electrochem. Soc. **147** (2000) 2044.

[16] J. G. Velasco, J. New Mater. Electrochem Sys. **3** (2000) 147.

[17] M. Mori, T. Isobe and M. Senna, Solid State Ionics **81** (1995) 157.

[18] P. Lavela, M. Conrad, A. Mrotzek, B. Harbrecht and J. L. Tirado, J. Alloys and Compd. **282** (1999) 93.

[19] M. D. Levi and D. Aurbach, J. Electroanal. Chem. **421** (1997) 79.

10

Figure Captions

Fig. 1 Typical Cyclic voltammogram (CV) of MnO_2 electrode in various concentration of aqueous NaOH electrolyte under identical conditions (scan rate: 25 $\mu v.s^{-1}$; potential limit: 0.2 to -0.5 V and back) (a) 2, (b) 5, (c) 7 and (d) 10 M. Effect of repeated voltammetric cycling on the current vs. potential profile of MnO_2 is observed in the figure. Cycle numbers are indicated in the respective plots.

Fig. 2 Cyclic voltammetric curves of MnO_2 electrode at the first cycle in a various concentration of aqueous NaOH electrolyte. Increasing the concentration of alkali electrolyte increases the current response until 7 M concentration and then decreased.

Fig. 3 Effect of scan rates on the redox behaviours of MnO_2 electrode on the first cycle in aqueous NaOH electrolyte (a) 25, (b) 50, (c) 100 and (d) 200 $\mu v.s^{-1}$. The cathodic (C1) and anodic (A1) peak potential difference and intensities between the two peaks increased with scan rate.

Fig. 4 Typical Cyclic voltammogram (CV) and its effect of degree of reduction on MnO_2 electrode in 5 M concentration of aqueous NaOH electrolyte (scan rate: 25 $\mu v.s^{-1}$; potential limit: 0.2 to -1.0 V and back; extended to second electron reduction). As the electron diffusion is slow at higher potentials the process becomes irreversible in nature.

Fig. 5 The 40th discharge-charge profile of Zn-MnO_2 cells using aqueous (a) 7 M, and (b) 5 M concentration of aqueous NaOH electrolyte under a constant current of 0.2 mA.
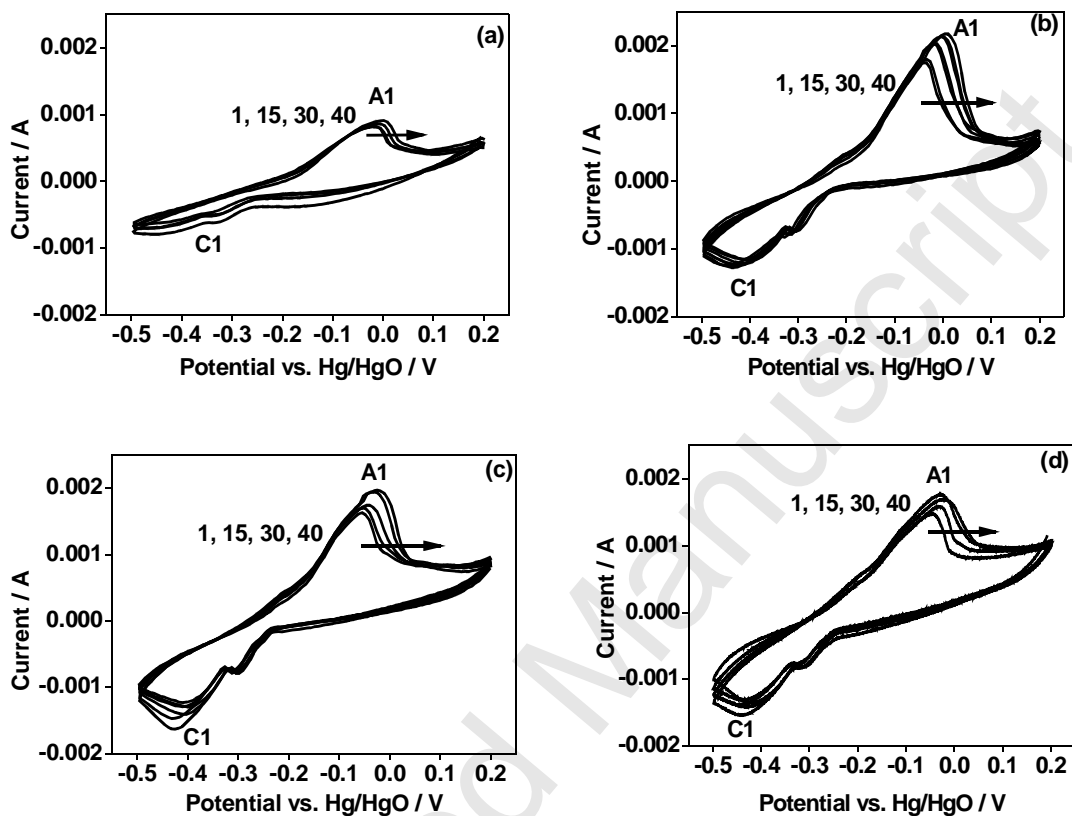
11

Fig. 1 Typical Cyclic voltammogram (CV) of MnO_2 electrode in various concentration of aqueous NaOH electrolyte under identical conditions (scan rate: 25 $\mu v.s^{-1}$; potential limit: 0.2 to -0.5 V and back) (a) 2, (b) 5, (c) 7 and (d) 10 M. Effect of repeated voltammetric cycling on the current vs. potential profile of MnO_2 is observed in the figure. Cycle numbers are indicated in the respective plots.
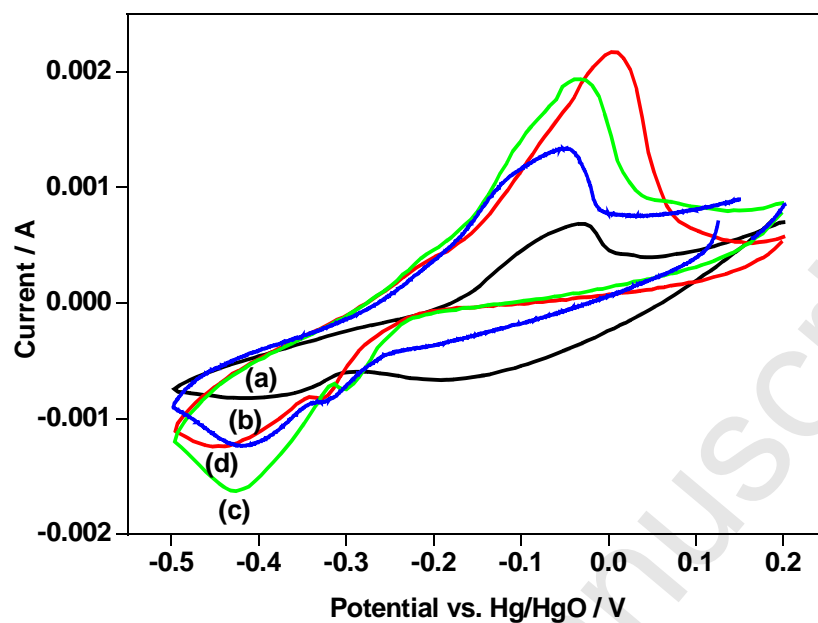
12

Fig. 2 Cyclic voltammetric curves of MnO_2 electrode at the first cycle in a various concentration of aqueous NaOH electrolyte. Increasing the concentration of alkali electrolyte increases the current response until 7 M concentration and then decreased.
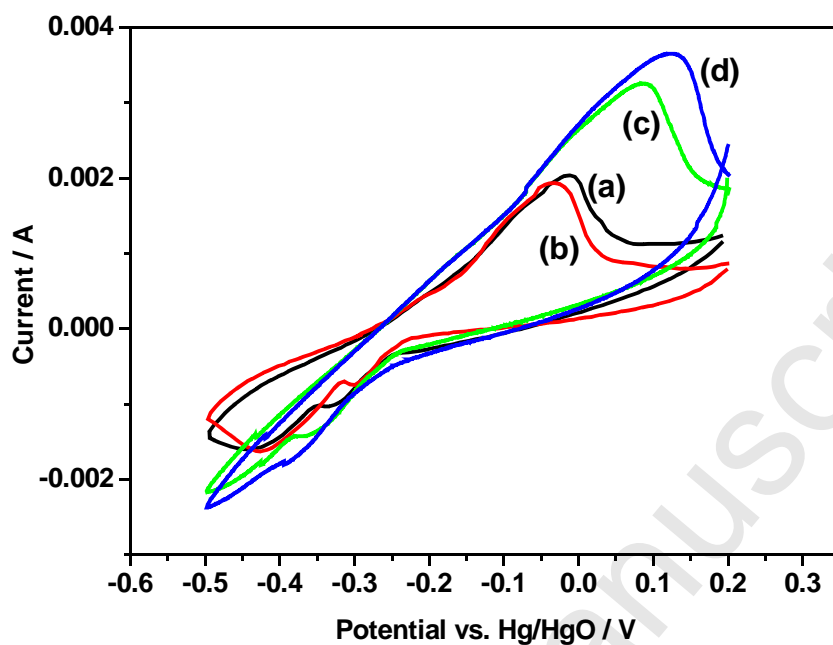
13

Fig. 3 Effect of scan rates on the redox behaviour of MnO_2 electrode on the first cycle in aqueous NaOH electrolyte (a) 25, (b) 50, (c) 100 and (d) 200 $\mu v.s^{-1}$. The cathodic (C1) and anodic (A1) peak potential difference and intensities between the two peaks increased with scan rate.
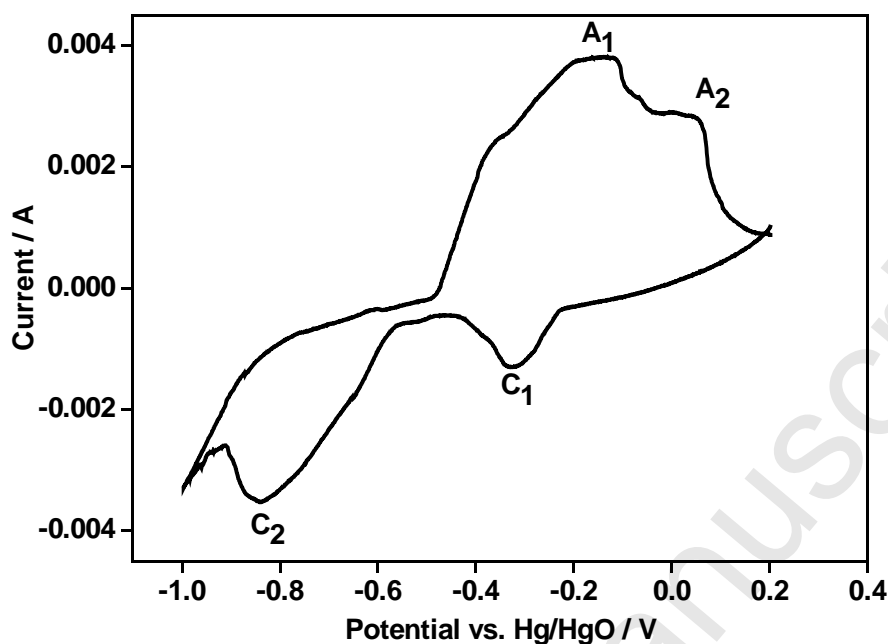
14

Fig. 4 Typical Cyclic voltammogram (CV) and its effect of degree of reduction on MnO_2 electrode in 5 M concentration of aqueous NaOH electrolyte (scan rate: 25 $\mu v.s^{-1}$; potential limit: 0.2 to -1.0 V and back; extended to second electron reduction). As the electron diffusion is slow at higher potentials the process becomes irreversible in nature.
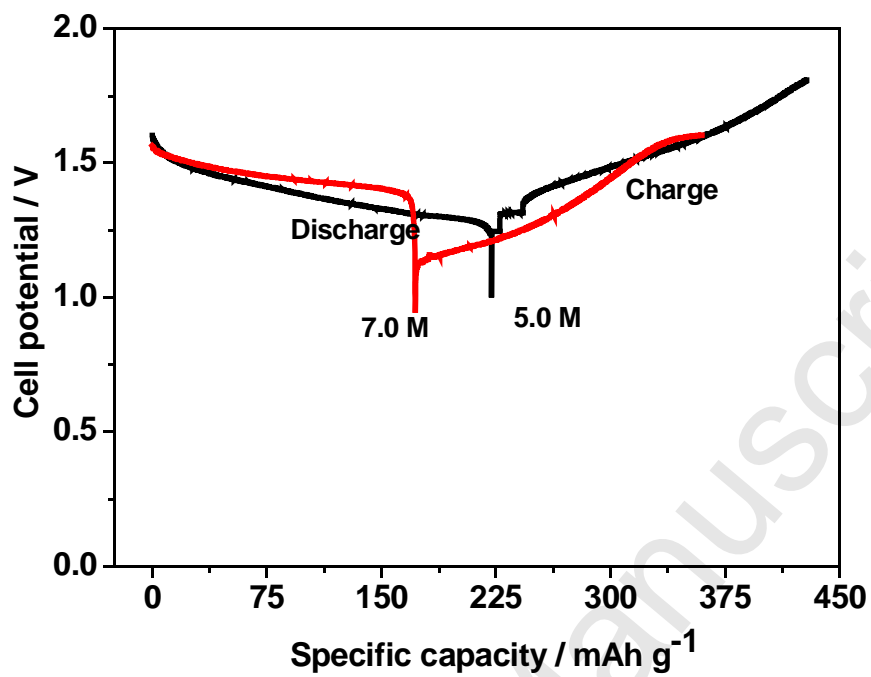
15

Fig. 5 The 40th discharge-charge profile of Zn-MnO$_2$ cells using aqueous (a) 7 and (b) 5 M concentration of aqueous NaOH electrolyte under a constant current of 0.2 mA.

16